## IV. Conclusions

The finite-element method for cylindrical polar geometries has been developed and applied to circular and sector waveguides to establish rates of convergence and absolute errors in cross sections with and without singular points. The mode structure of the double-ridged waveguide has been established for various symmetries and it is concluded that the waveguide has the advantages over the circular waveguide of 1) reduced cutoff frequency and wave impedance and 2) increased bandwidth. The most general type of waveguide in polar geometry directly solvable by this method has spiral boundaries. Examples of these have been given and particular cases studied. It is clear that other geometries not described here but nevertheless interesting might also be solved by the method. There is, for example, a whole class of problems involving coaxial structures where the solution of Laplace's or Helmholtz's equation might be required. This generalization of the usual finite-element method allows boundaries linear in an $r\theta$ coordinate system to be treated exactly and effectively removes from consideration the need to treat [11] truncation error at curved boundaries.

## References


[1] O. C. Zienkiewicz, *The Finite Element Method in Engineering Science*. London, England: McGraw-Hill, 1971.

[2] P. Silvester, "High-order polynomial triangular finite-element for potential problems," *Int. J. Eng. Sci.*, vol. 7, pp. 849–861, 1969.

[3] A. Wexler, "Computation of electromagnetic fields," *IEEE Trans. Microwave Theory Tech. (Special Issue on Computer-Oriented Microwave Practices)*, vol. MTT-17, pp. 416–439, Aug. 1969.

[4] J. Ergatoudis, B. M. Irons, and O. C. Zienkiewicz, "Curved isoparametric quadrilateral elements in finite element analysis," *Int. J. Solid Structures*, vol. 4, pp. 31–42, 1968.

[5] P. Daly, "Finite-elements for field problems in cylindrical coordinates," *Int. J. Num. Meth. Eng.*, vol. 6, no. 2, pp. 169–178, 1973.

[6] P. Daly and J. D. Helps, "Exact finite-element solutions to Helmholtz's equation," *Int. J. Num. Meth. Eng.*, vol. 6, no. 4, pp. 529–542, 1973.

[7] A. M. A. El-Sherbiny, "Cutoff wavelengths of ridged, circular, and elliptic guides," *IEEE Trans. Microwave Theory Tech.*, vol. MTT-21, pp. 7–12, Jan. 1973.

[8] M. Abramowitz and I. A. Stegun, *Handbook of Mathematical Functions*. New York: Dover, p. 18.

[9] ——, *Handbook of Mathematical Functions*. New York: Dover, p. 411.

[10] R. H. T. Bates and F. L. Ng, "Point matching computation of transverse resonances," *Int. J. Num. Meth. Eng.*, vol. 6, no. 2, pp. 155–168.

[11] D. J. Richards and A. Wexler, "Finite-element solutions within curved boundaries," *IEEE Trans. Microwave Theory Tech.*, vol. MTT-20, pp. 650–657, Oct. 1972.


# The Solution of Inhomogeneous Waveguide Problems Using a Transmission-Line Matrix

PETER B. JOHNS

***Abstract*—A method of applying the transmission-line matrix method to inhomogeneous waveguide structures is described. The technique uses open-circuit stubs of variable characteristic impedance at each node in the matrix, thereby providing an analog for a dielectric. LSE and LSM modes in rectangular waveguides, and problems involving a step of dielectric are solved. Results are given in terms of the cutoff frequency and field pattern for continuous waveguides, and the waveguide input impedance for scattering problems.**

## Introduction

THE transmission-line matrix method has been used to solve scattering problems in waveguides [1] and also to obtain the cutoff frequencies for waveguides of arbitrary cross section [2]. In both cases, the waveguides were assumed to be filled with a homogeneous medium. In applying the principles of the transmission-line matrix method to random walk analysis [3], results were obtained for a one-dimensional inhomogeneously filled waveguide. However, there is a large class of inhomogeneous waveguide problems that require solution in two space dimensions and an application technique for the transmission-line matrix method in such cases is introduced in this paper.

Manuscript received June 1, 1973; revised September 14, 1973.
The author is with the Department of Electrical and Electronic Engineering, University of Nottingham, Nottingham, England.

## Matrix Configuration and Properties

In [1] and [2], propagation in a two-dimensional medium is represented by the voltages and currents on a Cartesian mesh of TEM transmission lines. Analysis of the mesh is accomplished by considering an impulsive excitation and following the progress of impulses as they propagate throughout the matrix. The mesh is represented at each node by a submatrix of four numbers describing

the magnitude of the incident voltages along the four coordinate directions. The matrix as a whole consists of a number of submatrices corresponding to the number of nodes in the mesh. Thus, if the voltage impulses incident on a node at time $k$ are represented by

$$\begin{matrix} \\ \\ \\ \\ k \end{matrix}\begin{pmatrix} V_1 \\ V_2 \\ V_3 \\ V_4 \end{pmatrix}^i$$

and at time $k+1$, they become reflected pulses

$$\begin{matrix} \\ \\ \\ \\ k+1 \end{matrix}\begin{pmatrix} V_1 \\ V_2 \\ V_3 \\ V_4 \end{pmatrix}^r .$$

Then, in [1], it is shown that

$$\begin{matrix} \\ \\ \\ \\ k+1 \end{matrix}\begin{pmatrix} V_1 \\ V_2 \\ V_3 \\ V_4 \end{pmatrix}^r = \frac{1}{2}\begin{pmatrix} -1 & 1 & 1 & 1 \\ 1 & -1 & 1 & 1 \\ 1 & 1 & -1 & 1 \\ 1 & 1 & 1 & -1 \end{pmatrix}\begin{matrix} \\ \\ \\ \\ k \end{matrix}\begin{pmatrix} V_1 \\ V_2 \\ V_3 \\ V_4 \end{pmatrix}^i . \quad (1)$$

The reflected pulses from each node then become incident pulses on neighboring nodes and the process is repeated on an iterative basis. Each iteration corresponds to a unit of time which is the time required for pulses to travel from one node to its neighbor.

In the new matrix proposed, an additional length of line or stub is introduced to the mesh as shown in Fig. 1. The stubs are open circuit and of length $\Delta l/2$, where $\Delta l$ is the distance between nodes. They are of variable characteristic admittance ($Y_0$) relative to the unity characteristic admittance assumed for the main matrix of transmission lines. There are now five voltage pulses incident on each node, four from the lines as in the original formulation ($V_1$, $V_2$, $V_3$, and $V_4$), and one from the stub ($V_5$). Pulse analysis for each node gives the new version of (1) as

$$\begin{matrix} \\ \\ \\ \\ \\ k+1 \end{matrix}\begin{pmatrix} V_1 \\ V_2 \\ V_3 \\ V_4 \\ V_5 \end{pmatrix}^r = \frac{1}{Y_0+4}\begin{pmatrix} -(Y_0+2) & 2 & 2 & 2 & 2Y_0 \\ 2 & -(Y_0+2) & 2 & 2 & 2Y_0 \\ 2 & 2 & -(Y_0+2) & 2 & 2Y_0 \\ 2 & 2 & 2 & -(Y_0+2) & 2Y_0 \\ 2 & 2 & 2 & 2 & (Y_0-4) \end{pmatrix}\begin{matrix} \\ \\ \\ \\ \\ k \end{matrix}\begin{pmatrix} V_1 \\ V_2 \\ V_3 \\ V_4 \\ V_5 \end{pmatrix}^i . \quad (2)$$

Reflected pulses on the lines become incident pulses on neighboring nodes as before. The reflected pulse on the stub becomes the new incident pulse on the node from the stub, since the stub length is $\Delta l/2$ and pulses are reflected from the open circuit at the end.

At low frequencies, the effect of the stub is to add to each matrix node an additional lumped shunt capacitance of $CY_0\Delta l/2$. $C$ is the total shunt capacitance per unit length of the main matrix of lines that are of unity characteristic admittance. The total shunt capacitance at each node therefore becomes $2C\Delta l(1 + Y_0/4)$ and the low frequency velocity of waves on the matrix ($v_{n0}$) is given by

$$v_{n0}^2 = \frac{c^2}{2(1 + Y_0/4)} \quad (3)$$

where $c$ is the free space velocity of waves. Thus the velocity of waves on the matrix is now made variable simply by altering the value of the single constant $Y_0$.

As the frequency increases, the fact that the stub is a distributed capacitance and not lumped (as assumed above) becomes important. An exact analysis is needed to establish the range of frequencies over which (3) is sufficiently accurate. This is carried out by considering propagation of plane waves parallel to one of the matrix coordinates and diagonally across the matrix as in [1]. The following transmission equations connect the input voltages and currents ($V_i$ and $I_i$) with the output voltages and currents ($V_{i+1}$ and $I_{i+1}$) of one cell of the periodic structure involved. For propagation in the direction of one of the matrix coordinates the equation is

$$\begin{pmatrix} V_i \\ I_i \end{pmatrix} = \begin{pmatrix} \cos\theta/2 & j\sin\theta/2 \\ j\sin\theta/2 & \cos\theta/2 \end{pmatrix}\begin{pmatrix} 1 & 0 \\ 2j(1 + Y_0/2)\tan\theta/2 & 1 \end{pmatrix} \cdot \begin{pmatrix} \cos\theta/2 & j\sin\theta/2 \\ j\sin\theta/2 & \cos\theta/2 \end{pmatrix}\begin{pmatrix} V_{i+1} \\ I_{i+1} \end{pmatrix}.$$

For diagonal propagation, the equation becomes

$$\begin{pmatrix} V_i \\ I_i \end{pmatrix} = \begin{pmatrix} \cos\theta/2 & j\sin\theta/2 \\ j\sin\theta/2 & \cos\theta/2 \end{pmatrix}\begin{pmatrix} 1 & 0 \\ jY_0/2\tan\theta/2 & 1 \end{pmatrix} \cdot \begin{pmatrix} \cos\theta/2 & j\sin\theta/2 \\ j\sin\theta/2 & \cos\theta/2 \end{pmatrix}\begin{pmatrix} V_{i+1} \\ I_{i+1} \end{pmatrix}.$$

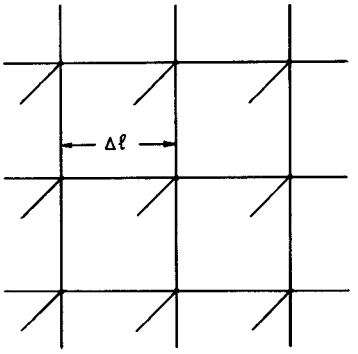


Fig. 1. Transmission-line matrix with open-circuit stubs.

In these equations

$$\theta = \frac{\omega \Delta l}{c} = \frac{2\pi \Delta l}{\lambda}.$$

The phase constant for the matrix ($\beta_n$) is therefore given by

$$\sin^2\left(\frac{\beta_n \Delta l}{2}\right) = 2(1 + Y_0/4)\sin^2\left(\frac{\omega \Delta l}{2c}\right) \tag{4}$$

for propagation in the direction of the matrix coordinates and

$$\sin^2\left(\frac{\beta_n \Delta l}{2}\right) = (1 + Y_0/4)\sin^2\left(\frac{\omega \Delta l}{2c}\right) \tag{5}$$

for diagonal propagation.

The velocity ($v_n$) of waves on the matrix relative to the free space velocity ($c$) for various values of $Y_0$ corresponding to (4) are plotted in Fig. 2. These characteristics show that as the low frequency velocity ($v_{n0}$) is reduced by the action of the stubs, so the usable frequency range also reduces. Cutoff always occurs first in the direction of the coordinates and is given by the expression

$$\left(\frac{\Delta l}{\lambda}\right)_{\text{cutoff}} = \frac{1}{\pi}\sin^{-1}\left(\frac{v_{n0}}{c}\right). \tag{6}$$

To cover a certain distance in a diagonal direction on the transmission-line matrix, the waves traveling along the component transmission lines have to cover $\sqrt{2}$ times the distance. However, (4) and (5) and Fig. 2 show that over a workable frequency range, the velocity of the waves

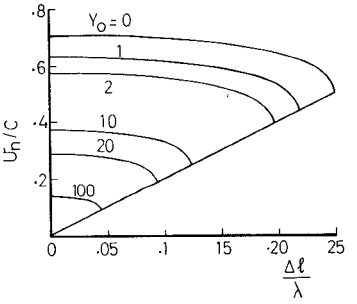


Fig. 2. Velocity characteristic for transverse waves on a stub loaded transmission-line matrix.

along the lines for a diagonally propagating wave is $\sqrt{2}$ times the value for waves propagating in the direction of the coordinates. Thus the effective velocities of the waves traveling in the two directions is the same. As the frequency increases, this relationship no longer holds, and velocity errors are introduced into the method. The maximum error from this cause may be calculated using (4) and (5) as shown in [2].

## The LSE Mode in a Rectangular Cavity

The simple inhomogeneous cavity of Fig. 3 is used to test the new matrix by obtaining the resonant frequency for the quasi-$H_{10}$ LSE mode. If the matrix stubs are merely thought of as additional lumped capacitance, then the line equations take their usual form [1], [2]:

$$\frac{\partial V_y}{\partial x} = -L\frac{\partial I_x}{\partial t}$$

$$\frac{\partial V_y}{\partial z} = -L\frac{\partial I_z}{\partial t}$$

$$\frac{\partial I_x}{\partial x} + \frac{\partial I_z}{\partial z} = -2C\frac{\partial V_y}{\partial t} \tag{7}$$

where

$$C = 1 + Y_0/4.$$

The appropriate expansion for Maxwell's equations for $\partial/\partial y = 0$ is

$$\frac{\partial E_y}{\partial x} = -\mu\frac{\partial H_z}{\partial t}$$

$$\frac{\partial E_y}{\partial z} = \mu\frac{\partial H_x}{\partial t}$$

$$\frac{\partial H_x}{\partial z} - \frac{\partial H_z}{\partial x} = \epsilon\frac{\partial E_y}{\partial t}. \tag{8}$$

Equivalences between line and field parameters may be made as usual and in particular the equivalence between $\epsilon$ and $2C$ is noted. Thus the problem of Fig. 3 is solved by applying the variable capacitance matrix (2) with admittances $Y_0$ assigned according to the position of nodes in the cavity. The results for 100 iterations of the matrix are shown in Table I for different lengths $L$ of the cavity with $\epsilon_r = 2.45$.

Terminating the output impulse function after 100 iterations introduces the possibility of a truncation error [2]

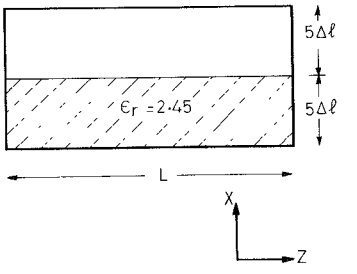


Fig. 3. Two-dimensional inhomogeneous cavity.

TABLE I
QUASI-$H_{10}$ LSE MODE IN RECTANGULAR GUIDE

| Cavity Length ($\Delta l$) | $\frac{\beta c}{\omega}$ | Numerical Result ($\Delta l/\lambda$) | Analytical Result ($\Delta l/\lambda$) | Error % | Maximum Truncation Error % | Maximum Velocity Error % |
|---|---|---|---|---|---|---|
| 5 | 1.265 | 0.078 1 | 0.079 1 | 1.3 | 0.4 | 2.0 |
| 6 | 1.198 | 0.069 2 | 0.069 6 | 0.6 | 0.6 | 1.6 |
| 7 | 1.134 | 0.062 5 | 0.063 0 | 0.8 | 0.8 | 1.2 |
| 10 | 0.964 | 0.051 8 | 0.051 8 | 0.0 | 1.2 | 0.9 |
| 20 | 0.602 | 0.041 3 | 0.041 5 | 0.5 | 1.8 | 0.5 |

$\epsilon_r = 2.45$.

and the table shows the maximum value this error can take. The worst velocity error occurs in the dielectric and its value, obtained from (4), is also shown in Table I.

## DIELECTRIC BOUNDARY CONDITIONS

In the example of the previous section, the $E$ field in the waveguide is equivalent to the voltage on the transmission-line matrix. The variable capacitance available on the matrix serves to provide a variable permittivity in the waveguide. The matrix therefore not only provides the correct velocity conditions for a dielectric but also gives the correct boundary conditions at the air–dielectric interface.

Sometimes it is necessary to make an $H$ field in the waveguide equivalent to the voltage on the transmission-line matrix and in this case the variable capacitance is equivalent to a variable permeability in the guide. Therefore, for a dielectric-loaded waveguide, the velocity of waves in the dielectric will still be correct, but the wave impedance will not. The intrinsic impedance of the waves on a matrix within a dielectric medium is a relative quantity and it is only at the boundary between two media that any correction is necessary. The correction may be achieved by introducing boundary transmission and reflection coefficients similar to those used in random walk techniques [3].

If, for waves on the matrix,

$$r = \frac{\text{intrinsic impedance of medium } 1}{\text{intrinsic impedance of medium } 2}$$

and if $\Gamma_{12}$ and $T_{12}$ are the voltage reflection and transmission coefficients of a pulse incident on medium 2 from medium 1, then

$$\Gamma_{21} = \frac{1 - r}{1 + r}$$

$$T_{21} = \frac{2}{1 + r}$$

$$\Gamma_{21} = \frac{r - 1}{r + 1}$$

$$T_{21} = \frac{2r}{r + 1}. \tag{9}$$

The cutoff frequency calculation for the quasi-$H_{10}$ LSE mode provides an example of the use of these coefficients. At cutoff, the waves propagate transversely and the problem can now be solved in the waveguide cross section. Strictly, the problem is one dimensional and the height of the guide in the $y$ direction is arbitrary. Fig. 4 shows the guide cross section in the $x$–$y$ plane and this time the $H_z$ field in the guide is equivalent to the voltage on the matrix. Since the capacitance is now equivalent to permeability, the intrinsic impedance of the waves in the slab is $\sqrt{2.45}$. The intrinsic impedance, however, is required to be $1/\sqrt{2.45}$. Correcting reflection and transmission coefficients on the matrix are therefore introduced according to (9) with $r = 1/2.45$.

Table II shows the result obtained, and it is compared with a similar calculation, but for a medium of $\mu_r = \sqrt{2.45}$ and $\epsilon_r = \sqrt{2.45}$. The velocity in such a medium is the same as in the previous case, but the impedance is matched to the air. The stub admittances for the dielectric are therefore the same, but the correcting reflection and transmission coefficients are for $r = 1/\sqrt{2.45}$.

Table II also shows the result for the cutoff of the dominant LSM mode ($\mu_r = 1$, $\epsilon_r = 2.45$) in square guide. This result was obtained without the use of boundaries of symmetry by exciting the guide with an $E$ field perpendicular to the dielectric–air interface and taking a similar field component for the solution.

## RESULTS FOR GUIDES WITH DIELECTRIC STEPS

The method is demonstrated by applying it to the waveguide configuration of Fig. 5. Results for the cutoff frequency of the dominant mode are shown in Table III

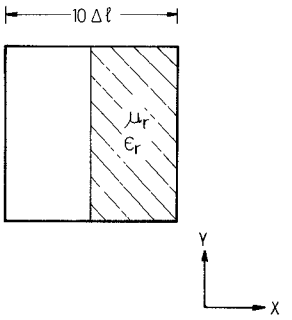


Fig. 4. Cross section of waveguide with dielectric slab.

TABLE II
CUTOFF OF LSE AND LSM MODES IN SQUARE WAVEGUIDE

| Mode | $\mu_r$ | $\epsilon_r$ | Numerical Result ($\Delta 1/\lambda$) | Analytical Result ($\Delta 1/\lambda$) |
|---|---|---|---|---|
| LSE | 1 | 2.45 | 0.037 21 | 0.037 30 |
| LSE | $\sqrt{2.45}$ | $\sqrt{2.45}$ | 0.038 89 | 0.038 98 |
| LSM | 1 | 2.45 | 0.038 38 | 0.038 50 |

Dimensions: 10Δ1; maximum velocity error: 0.5 percent. Five-hundred iterations of matrix.

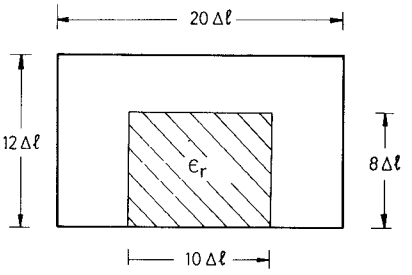


Fig. 5. Cross section of waveguide with dielectric ridge.

TABLE III
CUTOFF OF DOMINANT MODE IN DIELECTRIC RIDGE WAVEGUIDE

| $\epsilon_r$ | Numerical Result $\left[\frac{\omega a}{c}\right]$ | Results from Schlosser and Unger[4] $\left[\frac{\omega a}{c}\right]$ $\pm$ 0.01 (approx). | Maximum Velocity Error % |
|---|---|---|---|
| 2 | 1.303 | 1.31 | 0.1 |
| 3 | 1.176 | 1.18 | 0.2 |
| 4 | 1.102 | 1.11 | 0.2 |
| 6 | 1.012 | 1.02 | 0.3 |
| 8 | 0.968 | 0.98 | 0.3 |

Five-hundred iterations of matrix. $a = 10\Delta 1$.

and comparison is made with values obtained from curves calculated by Schlosser and Unger [4]. Since the dominant mode is an $H$-type mode (at cutoff), correcting transmission and reflection coefficients have been used at the dielectric boundaries. For the number of nodes chosen (120) the resulting values of $\Delta 1/\lambda$ are small (of the order of 0.01) and decrease in magnitude as $\epsilon_r$ increases. The velocity error is therefore small even for $\epsilon_r = 8$.

As indicated in [2], there is no difficulty in obtaining higher order modes using the transmission-line matrix method and the cutoff frequencies for these for $\epsilon_r = 2$ are shown in Table IV. Since the modes in dielectric loaded waveguide are a distorted version of those in a homogeneous guide, the mode classification of the latter is used to indicate the mode type.

The field configurations in Fig. 6 are calculated using the resonant frequency of a particular mode obtained from Table IV. The field solution is built up for every node on a cumulative basis after each iteration of the matrix. The computer storage required is somewhat less than usual since the impulse function for a particular node is not stored. The computer running time is slightly longer because of the additional trigonometrical calculations performed.

Finally, a two-dimensional waveguide problem involving diffraction at a dielectric step has been solved. In this case the propagation is down a waveguide as in [5], rather than across it. Fig. 7 shows frequency runs for the impedance, in magnitude and phase, looking into a dielectric loaded guide which is terminated in a discontinuity to free space impedance. Since the transmission-line matrix method is impulsive, all the points used to produce each of these curves were obtained from single sets of iterations of the matrix.

## DISCUSSION AND CONCLUSION

The transmission-line matrix method provides a means of obtaining the output impulse function at an observation point in a two-dimensional space in which wave propagation is taking place. This is achieved in the computer by storing the amplitude of pulses entering each node in a transmission-line matrix. With these amplitudes initially at zero, the matrix is then excited at selected source points with delta function pulses. As time progresses, pulses travel from one node to the next along the transmission lines and are transmitted and reflected at each node according to (2). Each iteration in the computer represents a time interval of $\Delta 1/c$, and the new values of the five incident impulse amplitudes for each node are calculated for each iteration. The network, therefore, becomes filled with pulses as waves spread out from the sources and are reflected at the boundaries. The output impulse function at a particular point in the matrix is simply obtained by observing the stream of pulses as they pass through the point in question. The solutions for all frequencies within the passband of the matrix are

| | | | | | | | | | |
|---|---|---|---|---|---|---|---|---|---|
| 40.5 | 39.0 | 37.6 | 35.2 | 31.7 | 27.1 | 22.0 | 16.2 | 9.8 | 3.3 |
| 40.7 | 39.3 | 38.0 | 35.3 | 32.0 | 27.4 | 22.3 | 16.4 | 10.0 | 3.4 |
| 41.1 | 39.8 | 38.5 | 36.1 | 32.5 | 28.0 | 22.7 | 16.7 | 10.2 | 3.4 |
| 41.7 | 40.6 | 39.3 | 37.0 | 33.6 | 28.9 | 23.4 | 17.2 | 10.5 | 3.5 |
| 42.5 | 41.4 | 40.3 | 38.2 | 35.4 | 30.9 | 24.9 | 16.2 | 11.1 | 3.7 |
| 43.3 | 42.3 | 41.2 | 39.3 | 36.8 | 32.4 | 26.4 | 19.3 | 11.7 | 4.0 |
| 44.1 | 43.1 | 42.1 | 40.3 | 38.0 | 33.8 | 27.4 | 20.1 | 12.5 | 4.2 |
| 44.8 | 43.9 | 43.0 | 41.1 | 38.8 | 34.6 | 28.1 | 20.8 | 12.8 | 4.3 |
| 45.4 | 44.6 | 43.6 | 41.6 | 39.4 | 35.3 | 28.8 | 21.3 | 13.0 | 4.5 |
| 45.9 | 45.1 | 44.1 | 42.1 | 39.9 | 35.8 | 29.2 | 21.6 | 13.3 | 4.7 |
| 46.3 | 45.3 | 44.4 | 42.5 | 40.3 | 35.9 | 29.4 | 22.0 | 13.4 | 4.6 |
| 46.5 | 45.4 | 44.5 | 42.7 | 40.5 | 36.2 | 29.6 | 21.9 | 13.5 | 4.7 |

(a)

| | | | | | | | | | |
|---|---|---|---|---|---|---|---|---|---|
| 0.9 | 2.8 | 4.3 | 5.5 | 6.0 | 6.7 | 6.5 | 5.6 | 3.5 | 1.3 |
| 2.9 | 8.3 | 13.0 | 16.9 | 19.0 | 20.2 | 18.7 | 15.5 | 10.2 | 3.6 |
| 4.5 | 13.2 | 21.1 | 27.7 | 31.4 | 33.5 | 31.4 | 26.0 | 17.2 | 6.1 |
| 5.9 | 17.4 | 28.0 | 37.1 | 42.9 | 46.5 | 44.3 | 37.0 | 24.6 | 8.6 |
| 6.9 | 20.7 | 33.8 | 44.9 | 52.8 | 59.8 | 58.0 | 48.0 | 31.9 | 11.0 |
| 7.0 | 22.0 | 36.7 | 49.1 | 59.3 | 67.6 | 65.8 | 54.8 | 36.0 | 11.9 |
| 7.7 | 32.2 | 38.0 | 50.9 | 61.3 | 70.9 | 69.4 | 58.0 | 38.6 | 13.6 |
| 7.4 | 22.3 | 36.1 | 48.5 | 58.8 | 68.0 | 66.5 | 55.4 | 36.8 | 13.0 |
| 6.5 | 19.5 | 31.5 | 42.2 | 51.0 | 59.2 | 58.2 | 48.6 | 32.3 | 11.4 |
| 4.8 | 15.0 | 24.5 | 32.8 | 39.3 | 36.1 | 45.3 | 37.8 | 25.3 | 8.9 |
| 2.7 | 9.3 | 15.6 | 20.5 | 24.6 | 29.7 | 28.9 | 24.2 | 15.9 | 5.4 |
| 1.0 | 3.4 | 5.5 | 7.1 | 8.1 | 10.0 | 10.0 | 8.3 | 5.6 | 2.0 |

(b)

Fig. 6. (a) Field pattern of $H_z$ for $H_{10}$ mode in dielectric ridge waveguide. (b) Field pattern of $E_z$ for $E_{21}$ mode in dielectric ridge waveguide.

now simultaneously available in this impulse function. For example, the impulse function for a closed structure (Fig. 5, for example) contains not only the resonant periodicity of the dominant mode but also the resonant periodicities for all higher order modes which are excited by the impulsive source. Similarly, for the impedance calculations of Fig. 7, the entire curves, both for magnitude and phase, are contained in a single impulse function.

TABLE IV
HIGHER ORDER MODES IN DIELECTRIC RIDGE WAVEGUIDE

| Mode | Numerical Result ($\Delta 1/\lambda$) |
|---|---|
| $TE_{10}$ | 0.020 73 |
| $TE_{01}$ | 0.035 77 |
| $TM_{11}$ | 0.037 21 |
| $TE_{20}$ | 0.044 51 |
| $TE_{11}$ | 0.045 07 |
| $TM_{21}$ | 0.053 49 |
| $TE_{21}$ | 0.058 44 |
| $TE_{30}$ | 0.065 63 |

$\epsilon_r = 2.0$. Five-hundred iterations of matrix.

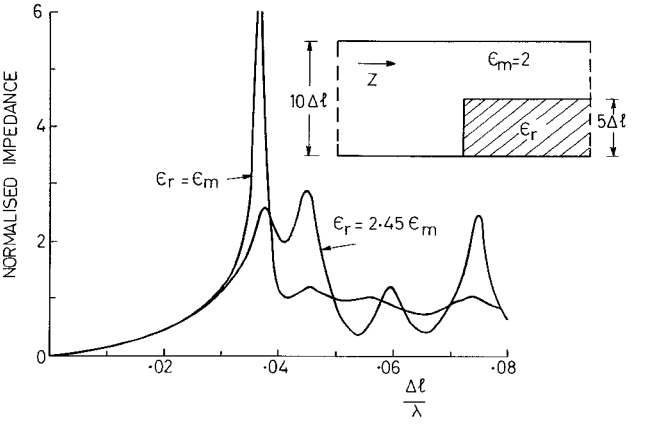


(a)

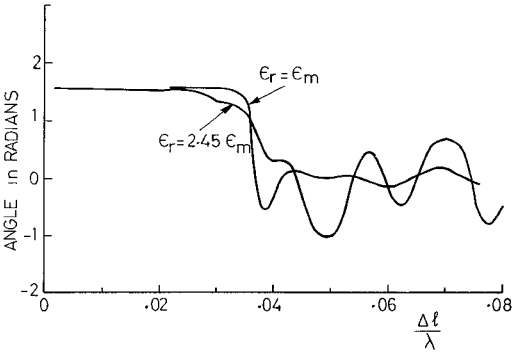


(b)

Fig. 7. (a) Magnitude of the impedance in a waveguide with a dielectric step. (b) Angle of the impedance in a waveguide with a dielectric step.

The required information is extracted from the output impulse function by taking the Fourier transform. Since the function consists of a series of regularly spaced discrete amplitudes, the transform is taken by a simple multiply-and-add routine in the computer.

Many of the numerical techniques currently available

for waveguide analysis are based on computer methods for solving analytical equations. This is often done by a variational approach as in the method of finite elements [6], [7] and the approach by English [8]. In these methods, the solution of a large number of simultaneous equations is required. This arises because some parameter of the formulation (such as frequency) is sought which enables all of the analytical equations to fit the boundary conditions simultaneously. By operating in the time domain, the solution of simultaneous equations is avoided, and there is no problem of convergence since a bound on the error for a given number of iterations may be calculated [2].

The accuracy of this method has been shown to compare favorably with the methods of finite elements and finite differences for homogeneous ridged waveguide in [2]. The accuracy of results in this application also compares favorably with the cutoff calculations for inhomogeneous waveguides by finite element analysis [7]. The process of taking the Fourier transform means that the field function between nodes is automatically circular, and it is this feature that accounts for the slightly better accuracy of this method compared with methods like finite differences and finite elements. Daly and Helps [9] have shown, for example, that the use of linear internodal functions limits the accuracy of finite elements and that increased accuracy may be obtained by the use of higher order polynomials.

In rectangular waveguides, the use of circular functions will, of course, give exact answers [2], but it would also seem that circular internodal functions give good results for waveguides with nonsinusoidal field distributions.

The calculation of higher order modes in the method of finite elements requires direct solution of the eigenvalue problem. In this case, the storage requirements for finite elements are considerably larger than for the transmission-line matrix method. For example, the transmission-line matrix method basically requires 5 numbers per node; the storage required for the $10 \times 12$ matrix of Fig. 5 is therefore 600 number locations. A further 500 locations is required to store the output impulse function. This means that calculations of this type may be carried out on a small computer. Computer running time is difficult to estimate but about 1 min of running time is required on a Honeywell DDP 516 computer in order to obtain a 500 iteration impulse function on a $10 \times 10$ matrix.

On the single matrix used here, account can only be taken of a voltage component and two current components which allows equivalences to be drawn for only three components in Maxwell's equations. The method therefore can only be used in cases where Maxwell's equations split into two independent sets of equations of three variables. Only calculations involving the general propagation of two-dimensional modes or the cutoff frequency of three-dimensional nodes can be performed. This is a disadvantage of this method compared to others. However, in many engineering applications the information provided by this method is useful, particularly since results for higher order modes are easily obtained. Also, the method of finite elements may not be a very convenient technique for calculating modes above cutoff. For this reason, the method of modal approximation [10] has been developed to use cutoff calculations made by the method of finite elements to obtain results above cutoff. In that the transmission-line matrix method obtains the cutoff frequency and the field values at cutoff for a mode, it may also be extended in this way.

The main advantage of the transmission-line matrix method over other methods is the ease with which it is formulated and programmed, and also the close relationship the method has with the actual mechanism of propagation. For example, the results of this paper, and for [1] and [2], have been calculated from a single universal program about 150 lines of Fortran, which accepts conduction and dielectric boundaries (for reasonably complicated geometries) as input data. The calculations have been performed on a 12 kbyte computer with no backing store. Also, the analogy between propagation on the matrix and propagation in free space has allowed loss calculations to be performed easily [11].

## References


[1] P. B. Johns and R. L. Beurle, "Numerical solution of 2-dimensional scattering problems using a transmission-line matrix," *Proc. Inst. Elec. Eng.*, vol. 118, pp. 1203–1208, Sept. 1971.

[2] P. B. Johns, "Application of the transmission-line method to homogeneous waveguides of arbitrary cross-section," *Proc. Inst. Elec. Eng.*, vol. 119, pp. 1086–1091, Aug. 1972.

[3] T. R. Rowbotham and P. B. Johns, "Waveguide analysis by random walks," *Electron. Lett.*, vol. 8, pp. 251–252, May 1972.

[4] W. Schlosser and H. G. Unger, *Advances in Microwaves*, vol. 1. New York: Academic, 1966, p. 339.

[5] E. G. Royer and R. Mittra, "The diffraction of electromagnetic waves by dielectric steps in waveguides," *IEEE Trans. Microwave Theory Tech.*, vol. MTT-20, pp. 273–279, Apr. 1972.

[6] Z. J. Csendes and P. Silvester, "Numerical solution of dielectric loaded waveguides: I—Finite-element analysis," *IEEE Trans. Microwave Theory Tech.*, vol. MTT-18, pp. 1124–1131, Dec. 1970.

[7] S. Ahmed and P. Daly, "Finite-element methods for inhomogeneous waveguides," *Proc. Inst. Elec. Eng.*, vol. 116, pp. 1661–1664, Oct. 1969.

[8] W. J. English, "Vector variational solutions of inhomogeneously loaded cylindrical waveguide structures," *IEEE Trans. Microwave Theory Tech.*, vol. MTT-19, pp. 9–18, Jan. 1971.

[9] P. Daly and J. D. Helps, "Exact finite-element solutions to Helmholtz's equation," *Int. J. Num. Meth. Eng.*, vol. 6, no. 4, pp. 529–542, 1973.

[10] Z. J. Csendes and P. Silvester, "Numerical solution to dielectric loaded waveguides: II—Modal approximation technique," *IEEE Trans. Microwave Theory Tech.*, vol. MTT-19, pp. 504–509, June 1971.

[11] S. Akhtarzad and P. B. Johns, "Transmission-line matrix solution of waveguides with wall losses," *Electron. Lett.*, vol. 9, pp. 335–336, July 1973.